Nonreciprocal heat flux via synthetic fields in linear quantum systems

Svend-Age Biehs [*]
Institut für Physik, Carl von Ossietzky Universität, 26111 Oldenburg, Germany;
Center for Nanoscale Dynamics, Carl von Ossietzky Universität, 26129 Oldenburg, Germany;
and Laboratoire Charles Coulomb, UMR No. 5221, CNRS, University of Montpellier, 34095 Montpellier, France

Pablo Rodriguez-Lopez [†]
Área de Electromagnetismo and Grupo Interdisciplinar de Sistemas Complejos,
Universidad Rey Juan Carlos, 28933 Móstoles, Madrid, Spain and Laboratoire Charles Coulomb, UMR No. 5221, CNRS,
University of Montpellier, 34095 Montpellier, France

Mauro Antezza [‡]
Laboratoire Charles Coulomb, UMR No. 5221, CNRS, University of Montpellier, 34095 Montpellier, France
and Institut Universitaire de France, 1 Rue Descartes, 75231 Paris Cedex 05, France

Girish S. Agarwal [§]
Institute for Quantum Science and Engineering, Department of Biological and Agricultural Engineering,
and Department of Physics and Astronomy, Texas A&M University, College Station, Texas 77845, USA

(Received 12 June 2023; accepted 18 September 2023; published xxxxxxxxxx)

We study the heat transfer between N coupled quantum resonators with applied synthetic electric and magnetic fields realized by changing the resonator parameters by external drivings. To this end we develop two general methods, based on the quantum optical master equation and on the Langevin equation for N coupled oscillators where all quantum oscillators can have their own heat baths. The synthetic electric and magnetic fields are generated by a dynamical modulation of the oscillator resonance with a given phase. Using Floquet theory, we solve the dynamical equations with both methods, which allow us to determine the heat flux spectra and the transferred power. We apply these methods to study the specific case of a linear tight-binding chain of four quantum coupled resonators. We find that, in that case, in addition to a nonreciprocal heat flux spectrum already predicted in previous investigations, the synthetic fields induce here nonreciprocity in the total heat flux, hence realizing a net heat flux rectification.

DOI: 10.1103/PhysRevA.00.002200

I. INTRODUCTION

In the past decade a great number of experiments have verified the near-field enhancement of thermal radiation between two macroscopic objects down to distances of a few nanometers [1–9]. In particular, the theoretically proposed effects of thermal rectification with a phase-change diode [10,11], a phase-change material-based memory [12], and active heat flux switching or modulations [13–15] have been realized experimentally. Also, several proposals for heat flux rectification in nonreciprocal systems, called nonreciprocal heat flux, have been made, but these effects have not been demonstrated experimentally. Typically, these proposals rely on the application of magnetic fields to nanoscale setups involving magneto-optical materials or by using Weyl semimetals with intrinsic nonreciprocal optical properties. It can be shown theoretically that by means of magnetic fields the magnitude of the heat flux and its direction can be manipulated [16–23]. Due to the broken time-reversal symmetry, also nonreciprocal heat fluxes can exist in such cases, leading to persistent heat currents and fluxes [24,25], persistent angular momenta and spins [25–27], normal and anomalous Hall effects for thermal radiation [28,29], diode effects by coupling to nonreciprocal surface modes [30–33], and spin-directional near- and far-field thermal emission [34,35]. A tradeoff of using magneto-optical materials is that to have observable nonreciprocal heat fluxes, experiments with large magnetic fields in a nanoscale setup are necessary. On the other hand, using Weyl semimetals with intrinsic nonreciprocity does not allow for dynamic tuning.

Recently, the modulation of resonance frequencies of a system of resonators with a single modulation frequency but different phases has been interpreted as a way to create synthetic electric and magnetic fields [36]. For the energy transmission in a setup of two resonators with applied synthetic electric and magnetic fields, i.e., with a modulation of the resonance frequencies and a phase shift, it could be shown experimentally and theoretically that monochromatic waves

[*]s.age.biehs@uol.de
[†]pablo.ropez@urjc.es
[‡]mauro.antezza@umontpellier.fr
[§]girish.agarwal@tamu.edu

are transmitted in a nonreciprocal manner [37] if there is a nonzero phase shift, i.e., a synthetic magnetic field. If the two resonators with applied synthetic electric and magnetic fields are coupled to two thermal reservoirs within a master-equation approach [38–41], then the transmission coefficients for the heat current in both directions are not the same, which is a manifestation of a broken detailed balance [42]. However, in this case the total power transferred between both resonances is reciprocal even in the presence of synthetic electric and magnetic fields [42].

That the transferred power is reciprocal might not be surprising for two reasons. First of all, in the context of Rytov's fluctuational electrodynamics it can easily be shown that the total radiative heat flux between two objects is always reciprocal [16]. Nonreciprocal effects necessitate at least a third object and nonreciprocal material properties of the objects or environment [43,44]. Another argument is that within the quantum master-equation approach for linearly coupled oscillators, typically nonlinear effects need to be included to have nonreciprocal heat flow [45], even though it seems that nonreciprocal heat flow can also be generated by specific choices of temperatures in a linear chain of oscillators [46,47]. However, as we will show below, the application of synthetic electric and magnetic fields can indeed generate nonreciprocal heat flow in a tight-binding configuration of four coupled resonators without the need for nonlinearity due to the presence of the synthetic magnetic field.

We distinguish our work from previous studies. Several kinds of modulations have been proposed such as the periodic modulation of the permittivity [48–50]. Such modulations have been shown to introduce synthetic magnetic fields for photons [51] and consequently related effects like the Aharonov-Bohm effect for photons [52]. In the context of thermal radiation, it could be demonstrated that permittivity modulations can introduce nonreciprocity, which manifests in a breakdown of the detailed balance in Kirchhoff's law [53] and can be employed for photonic refrigeration [54]. In similar approaches a combined dynamical modulation of the resonances of heat exchanging objects and their interaction strength was applied, resulting in a heat pumping effect and nonreciprocal heat fluxes in a three-resonator configuration [55,56]. Heat pumping effects also exist when only the interaction strengths in three-body configurations are dynamically modulated [57]. It must be emphasized that these effects are different from the heat shuttling effect where the temperature or chemical potentials of two reservoirs are periodically modulated around their equilibrium values in order to have a heat transport despite the fact that the system is on average in equilibrium [58–60]. Indeed, in that case the modulation affects the baths only and not resonator parameters. Finally, it could be demonstrated theoretically that geometrical phases by adiabatic dynamical modulation of resonators with nonreciprocal conductance can increase or reduce the thermal relaxation [61] and rapid magnetic-field modulations in magneto-optical systems can substantially increase the cooling [62].

In this work we extend the quantum Langevin equation (QLE) and quantum master equation (QME) approach used in Ref. [42] to the case of N coupled arbitrary resonators with their own heat baths as sketched in Fig. 1 with applied synthetic electric and magnetic fields. Both methods can be used to calculate the heat flux between any two resonators which are coupled to their own reservoirs. We show numerically that both methods give the same values for the heat flux. The QLE approach naturally allows for calculating the heat flux spectra, whereas the master-equation method is a better choice for fast numerical calculations of the heat flux. We use both methods to show that the heat flux itself is nonreciprocal in the presence of synthetic fields in a linear tight-binding chain of four resonators. This finding might be of great interest in the field of quantum thermodynamics, where energy flux management and thermal tasks in many-body quantum systems are of high relevance as in the studies on long-range transport and amplification in chains of atoms and ions [63,64], distributed thermal tasks in many-body systems [65], chiral or nonlocal heat transport [66,67], quantum fluctuation theorems [68], thermodynamical consistency of master equations [69], and many others.

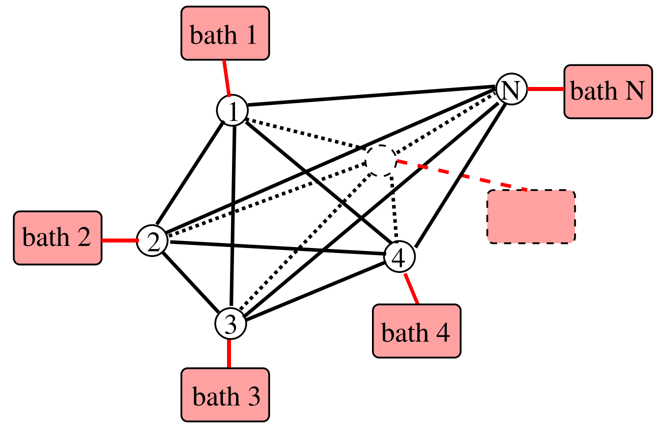

FIG. 1. Sketch of N coupled quantum resonators, each coupled to its own heat bath.

The paper is organized as follows. First, in Sec. II we introduce the standard master equation for N coupled resonators with N reservoirs. We derive the dynamical equations for the mean values of products of the resonator amplitudes and introduce the QLE for the coupled resonator system. In Sec. III we introduce the synthetic fields in the QLE approach and provide a formal solution in Fourier space. In Sec. IV we introduce the synthetic fields in the master-equation approach and give a formal solution by making a Fourier series ansatz. In Sec. V we show the occurrence of nonreciprocal heat flux in the presence of synthetic electric and magnetic fields in a four-resonator chain. We conclude with a summary in Sec. VI.

II. LANGEVIN AND MASTER EQUATIONS

We start by writing the Hamiltonian of a coupled harmonic-oscillator system (each oscillator coupled to its own heat bath of oscillators), which is given by [70,71],

$$H = H_S + \sum_i H_{B,i} + \sum_i H_{SB,i}, \tag{1}$$

with the Hamiltonian of the system of coupled oscillators

$$H_S = \sum_i \hbar\omega_i a_i^\dagger a_i + \sum_{i,j,i\neq j} \hbar g_{ij} a_i^\dagger a_j, \tag{2}$$

with resonance frequencies ω_i and coupling constants $g_{ij} = g_{ji}^*$ for the Hermitian system $H_S^\dagger = H_S$ and the bosonic creation and annihilation operators $a_i^\dagger$ and a_i, respectively. The bath oscillator Hamiltonians are given by ($i = 1, \dots, N$)

$$H_{B,i} = \sum_j \hbar\omega_{ij} b_{ij}^\dagger b_{ij}, \tag{3}$$

with bosonic creation and annihilation operators $b_{ij}^\dagger$ and b_{ij}, respectively, and the Hamiltonians describing the linear coupling between the system oscillators and their baths are given by

$$H_{SBi} = i\hbar \sum_j g_{B,ij}(a_i + a_i^\dagger)(b_{ij} - b_{ij}^\dagger), \tag{4}$$

with the corresponding coupling constants $g_{B,ij}$. By assuming the validity of the Born-Markov and rotating-wave approximation and tracing out the bath variables we can arrive at the QME [71]

$$\begin{aligned}\frac{\partial \rho_S}{\partial t} &= -i\sum_i \omega_i [a_i^\dagger a_i, \rho_S] \\ &\quad - i\sum_{i,j;i\neq j} g_{ij}[a_i^\dagger a_j, \rho_S] \\ &\quad - \sum_i \kappa_i (n_i+1)(a_i^\dagger a_i \rho_S - 2a_i\rho_S a_i^\dagger + \rho_S a_i^\dagger a_i) \\ &\quad - \sum_i \kappa_i n_i (a_i a_i^\dagger \rho_S - 2a_i^\dagger \rho_S a_i + \rho_S a_i a_i^\dagger),\end{aligned} \tag{5}$$

where the coupling to the bath oscillators is formally given in terms of the coupling constants $\kappa_i = \pi\sum_j g_{B,ij}^2 \delta(\omega_{ij} - \omega_i)$ and $n_i = [\exp(\hbar\omega_i/k_B T_i) - 1]^{-1}$ are the mean occupation numbers at the bath temperatures T_i. As mentioned before, g_{ij} is in general a complex number with the constraint $g_{ij} = g_{ji}^*$ to ensure Hermiticity of H_S. This master equation is also called the local approach and it is valid when the intersystem coupling does not affect the system-bath coupling [41,72,73].

From the QME we can derive the dynamical equation for the mean values of any observable. For example, for the mean values of products of raising and lowering operators we obtain the set of equations ($k, l = 1, \dots, N; k \neq l$)

$$\begin{aligned}\frac{d}{dt}\langle a_k^\dagger a_k\rangle &= -i\sum_{j,j\neq k}(g_{kj}\langle a_k^\dagger a_j\rangle - g_{jk}\langle a_k a_j^\dagger\rangle) \\ &\quad - 2\kappa_k\langle a_k^\dagger a_k\rangle + 2\kappa_k n_k,\end{aligned} \tag{6}$$

$$\begin{aligned}\frac{d}{dt}\langle a_k^\dagger a_l\rangle &= \Omega_{kl}\langle a_k^\dagger a_l\rangle - i\sum_{j\neq k; j\neq l}(g_{lj}\langle a_k^\dagger a_j\rangle - g_{jk}\langle a_j^\dagger a_l\rangle) \\ &\quad - i g_{lk}(\langle a_k^\dagger a_k\rangle - \langle a_l^\dagger a_l\rangle),\end{aligned} \tag{7}$$

with

$$\Omega_{kl} = i(\omega_k - \omega_l) - \kappa_k - \kappa_l. \tag{8}$$

In the following we will refer to this set of equations for the mean values of operator products (6) and (7) as the master-equation approach as they are derived from the QME (5).

Similarly, we obtain for the time evolution of the mean values of the raising and lowering operators of each oscillator a_i the set of equations ($k = 1, \dots, N$)

$$\frac{d}{dt}\langle a_k\rangle = -\Omega_k\langle a_k\rangle - i\sum_{i;i\neq k} g_{ki}\langle a_i\rangle, \tag{9}$$

with $\Omega_k \equiv i\omega_k + \kappa_k$. The set of equations for the mean values of the lowering operators of the two oscillators in Eq. (9) motivates the introduction of a set of QLE for the operators themselves instead of their expectation values

$$\dot{a}_k = -i\omega_k a_k - \kappa_k a_k - i\sum_{i,i\neq k} g_{ki} a_i + F_k, \tag{10}$$

where the coupling to baths is taken into account by the bath operators F_k, which obviously must fulfill $\langle F_k\rangle = 0$ to retrieve Eq. (9). To be consistent with the QME approach and in particular with the set of equations (6) and (7), the correlation functions of the bath operators are given by

$$\langle F_k^\dagger(t) F_k(t')\rangle = 2\kappa_k n_k \delta(t - t'), \tag{11}$$

$$\langle F_k(t) F_k^\dagger(t')\rangle = 2\kappa_k (n_k + 1)\delta(t - t'), \tag{12}$$

and $\langle F_k F_k\rangle = \langle F_k^\dagger F_k^\dagger\rangle = 0$. Furthermore, the bath operators of different baths are uncorrelated. Here the δ function in time is due to the Markov assumption, whereas the prefactors (or diffusion terms) can be derived from the QME with the method used in Ref. [74]. Hence, the QLE approach is related via (5) to the QME approach, so both approaches are equivalent descriptions but on different levels. The QLE approach will allow us to determine the heat flux spectra, whereas the QME approach is a faster method for a direct computation of the full heat flux.

III. LANGEVIN EQUATIONS WITH SYNTHETIC FIELDS

We now use the set of QLEs as introduced above and include a frequency modulation ($k = 1, \dots, N$)

$$\omega_k \to \omega_k + m_k\beta\cos(\Omega t + \theta_k), \tag{13}$$

with phase shifts θ_k and $m_k = \{0, 1\}$ (for $m_k = 0$ the modulation of oscillator k is turned off and for $m_k = 1$ the modulation is turned on). The set of coupled QLEs in frequency space is therefore ($k = 1, \dots, N$)

$$X_k a_k(\omega) + i\sum_{l\neq k} g_{kl} a_l(\omega) = F_k + \frac{\beta}{2i}(a_{k,-}e^{-i\theta_k} + a_{k,+}e^{+i\theta_k}), \tag{14}$$

introducing

$$X_k = i(\omega_k - \omega) + \kappa_k \tag{15}$$

and the shorthand notation

$$a_{k,\pm} = a_k(\omega \pm \Omega). \tag{16}$$

The coupled QLEs can now be put in matrix form

$$\boldsymbol{\psi} = \mathbb{M}\mathbf{F} + \frac{\beta}{2i}\mathbb{M}\mathbb{Q}_+\boldsymbol{\psi}_+ + \frac{\beta}{2i}\mathbb{M}\mathbb{Q}_-\boldsymbol{\psi}_- \tag{17}$$

by introducing the vectors

$$\boldsymbol{\psi} = \begin{pmatrix} a_1(\omega) \\ \vdots \\ a_N(\omega) \end{pmatrix}, \quad \boldsymbol{\psi}_\pm = \begin{pmatrix} a_1(\omega \pm \Omega) \\ \vdots \\ a_N(\omega \pm \Omega) \end{pmatrix}, \quad \mathbf{F} = \begin{pmatrix} F_1(\omega) \\ \vdots \\ F_N(\omega) \end{pmatrix} \tag{18}$$

and the matrices

$$\mathbb{M} = \mathbb{A}^{-1}, \quad \text{with } \mathbb{A} = \begin{pmatrix} X_1 & ig_{12} & \cdots & ig_{1N} \\ ig_{21} & X_2 & \cdots & ig_{2N} \\ \vdots & \cdots & \vdots & \vdots \\ ig_{N1} & g_{N2} & \cdots & X_N \end{pmatrix}, \tag{19}$$

and

$$\mathbb{Q}_\pm = \mathrm{diag}(e^{\pm i\theta_1} m_1, \ldots, e^{\pm i\theta_N} m_N). \tag{20}$$

In Eq. (17) it can be clearly seen that due to the modulation there are couplings to the next sidebands $\omega \pm \Omega$ so that this set of equations is recursive and infinitely large. These sidebands can be understood as being the consequence of a synthetic constant electric field. Furthermore, the phase shift adds a phase $\pm\theta_k$ to this coupling which can be understood as a consequence of a synthetic magnetic field.

The solution of the coupled QLEs (17) can formally be written for all orders. By introducing the block vectors

$$\underline{\boldsymbol{\psi}} = (\ldots, \boldsymbol{\psi}_{++}, \boldsymbol{\psi}_+, \boldsymbol{\psi}, \boldsymbol{\psi}_-, \boldsymbol{\psi}_{--}, \ldots)^\mathsf{T}, \tag{21}$$

$$\underline{\mathbf{F}} = (\ldots, \mathbf{F}_{++}, \mathbf{F}_+, \mathbf{F}, \mathbf{F}_-, \mathbf{F}_{--}, \ldots)^\mathsf{T}, \tag{22}$$

the diagonal block matrix

$$\underline{\mathbb{M}} = \begin{pmatrix} \cdots & \cdots & \cdots & \cdots & \cdots \\ \cdots & \mathbb{M}_+ & \mathbb{O} & \mathbb{O} & \cdots \\ \cdots & \mathbb{O} & \mathbb{M} & \mathbb{O} & \cdots \\ \cdots & \mathbb{O} & \mathbb{O} & \mathbb{M}_- & \cdots \\ \cdots & \cdots & \cdots & \cdots & \cdots \end{pmatrix}, \tag{23}$$

and the tridiagonal block matrix

$$\underline{\mathbb{L}} = \begin{pmatrix} \cdots & \cdots & \cdots & \cdots & \cdots \\ \frac{i\beta}{2}\mathbb{M}_+\mathbb{Q}_+ & \mathbb{1} & \frac{i\beta}{2}\mathbb{M}_+\mathbb{Q}_- & \mathbb{O} & \cdots \\ \cdots & \frac{i\beta}{2}\mathbb{M}\mathbb{Q}_+ & \mathbb{1} & \frac{i\beta}{2}\mathbb{M}\mathbb{Q}_- & \cdots \\ \cdots & \mathbb{O} & \frac{i\beta}{2}\mathbb{M}_-\mathbb{Q}_+ & \mathbb{1} & \frac{i\beta}{2}\mathbb{M}_-\mathbb{Q}_- \\ \cdots & \cdots & \cdots & \cdots & \cdots \end{pmatrix}, \tag{24}$$

we can rewrite the coupled QLE (17) as a matrix equation

$$\underline{\mathbb{L}}\underline{\boldsymbol{\psi}} = \underline{\mathbb{M}}\underline{\mathbf{F}}. \tag{25}$$

Hence

$$\underline{\boldsymbol{\psi}} = \underline{\mathbb{L}}^{-1}\underline{\mathbb{M}}\underline{\mathbf{F}}. \tag{26}$$

By considering only block vectors $\underline{\boldsymbol{\psi}}$ of $2n+1$ vectors $\boldsymbol{\psi}$ with the corresponding block matrices of size $(2n+1) \times (2n+1)$ submatrices, we obtain the perturbation results up to order n. Note that the full size of the block vectors and matrices is $N(2n+1)$ and $N^2(2n+1)^2$, respectively.

To evaluate these spectra in our general formalism, we start with Eq. (26) and introduce the block matrices $\underline{\mathbb{Y}}_1 = \mathrm{diag}(1, 0, \ldots, 0, 1, 0, 0, \ldots)$, $\underline{\mathbb{Y}}_2 = \mathrm{diag}(0, 1, 0, \ldots, 0, 1, 0, 0, \ldots)$, $\underline{\mathbb{Y}}_3 = \mathrm{diag}(0, 0, 1, 0, \ldots, 0, 1, 0, 0, \ldots)$, etc., so that there are $N-1$ zeros between the nonzero entries and $\sum_k \underline{\mathbb{Y}}_k = \underline{\mathbb{1}}$. These matrices allow us to split the contributions from all baths k so that

$$\underline{\boldsymbol{\psi}} = \sum_{k=1}^{N} \underline{\mathbb{L}}^{-1}\underline{\mathbb{M}}\mathbb{Y}_k\underline{\mathbf{F}}. \tag{27}$$

To evaluate products, we use the fluctuation-dissipation theorem in the form

$$\langle F_k^\dagger(\omega + l\Omega)F_{k'}(\omega' + l'\Omega)\rangle = \delta_{k,k'}\delta_{l,l'}2\pi\delta(\omega - \omega')\langle F_k^\dagger F_k\rangle_\omega, \tag{28}$$

where $\langle F_k^\dagger F_k\rangle_\omega = 2\kappa_k n_k$. Here, in agreement with the treatment in the QME approach, we are assuming that n_k is constant, as demanded by the assumption of white noise. This assumption is justified for $\beta \ll \omega_k$ and $\Omega \ll k_\mathrm{B}T/\hbar$. Then we have

$$\langle \underline{\boldsymbol{\psi}}_\alpha^\dagger \underline{\boldsymbol{\psi}}_\epsilon \rangle_\omega = \sum_{k=1}^{N} 2\kappa_k n_k (\underline{\mathbb{L}}^{-1}\underline{\mathbb{M}}\underline{\mathbb{Y}}_k\underline{\mathbb{M}}^\dagger\underline{\mathbb{L}}^{-1\dagger})_{\epsilon,\alpha}, \tag{29}$$

using the properties $\underline{\mathbb{Y}}_k^\dagger = \underline{\mathbb{Y}}_k$ and $\underline{\mathbb{Y}}_k\underline{\mathbb{Y}}_k = \underline{\mathbb{Y}}_k$. From this expression we can numerically calculate all spectral correlation functions.

As detailed in Appendix B, the total power emitted by the hot oscillator or reservoir k into the system is given by [41,45]

$$P_k^\mathrm{em} = \int \frac{d\omega}{2\pi}\hbar\omega_k 2\kappa_k(n_k - \langle a_k^\dagger a_k\rangle_\omega). \tag{30}$$

Assuming that only reservoir k has nonzero temperature, then the heat flux flowing into the reservoir l is given by

$$P_{k\to l} = \int \frac{d\omega}{2\pi}\hbar\omega_l 2\kappa_l\langle a_l^\dagger a_l\rangle_\omega, \tag{31}$$

where $\langle a_l^\dagger a_l\rangle_\omega$ is given by $\langle \underline{\boldsymbol{\psi}}_\alpha^\dagger \underline{\boldsymbol{\psi}}_\epsilon \rangle_\omega$ from Eq. (29) with $\epsilon = \alpha = Nn + l$ coming from the term involving n_k due to bath k.

IV. MASTER EQUATIONS WITH SYNTHETIC FIELDS

Now, instead of the QLEs we use the QMEs (6) and (7) with periodic driving as in Eq. (13). This directly leads to the set of equations

$$\frac{d}{dt}\langle a_k^\dagger a_k\rangle = -i\sum_{j,j\neq k}(g_{kj}\langle a_k^\dagger a_j\rangle - g_{jk}\langle a_k a_j^\dagger\rangle) - 2\kappa_k\langle a_k^\dagger a_k\rangle + 2\kappa_k n_k, \tag{32}$$

$$\frac{d}{dt}\langle a_k^\dagger a_l\rangle = \tilde{\Omega}_{kl}\langle a_k^\dagger a_l\rangle - i\sum_{j\neq k;j\neq l}(g_{lj}\langle a_k^\dagger a_j\rangle - g_{jk}\langle a_j^\dagger a_l\rangle) - ig_{lk}(\langle a_k^\dagger a_k\rangle - \langle a_l^\dagger a_l\rangle), \tag{33}$$

with

$$\tilde{\Omega}_{kl} = i(\omega_k - \omega_l) - \kappa_k - \kappa_l + i\beta[m_k\cos(\Omega t + \theta_k) - m_l\cos(\Omega t + \theta_l)]. \tag{34}$$

To solve the equations, we make the Fourier series ansatz for the expectation values of each observable O such that

$$\langle O\rangle = \sum_n e^{-in\Omega t}\langle O\rangle_n. \tag{35}$$

Then we note that

$$\sum_n e^{-in\Omega t}\langle O\rangle_n[\cos(\Omega t + \theta_k) - \cos(\Omega t + \theta_l)] = \sum_n e^{-in\Omega t}\left(\frac{\eta_{kl}}{2}\langle O\rangle_{n+1} + \frac{\eta_{kl}^*}{2}\langle O\rangle_{n-1}\right), \tag{36}$$

with

$$\eta_{kl} = (m_k e^{i\theta_k} - m_l e^{i\theta_l}). \tag{37}$$

Inserting this ansatz into the set of equations (32) and (33) gives the following set of equations for the Fourier components:

$$(-in\Omega + 2\kappa_k)\langle a_k^\dagger a_k\rangle_n = -i\sum_{j,j\neq k}(g_{kj}\langle a_k^\dagger a_j\rangle_n - g_{jk}\langle a_k a_j^\dagger\rangle_n) + 2\kappa_k n_k\delta_{n0}, \tag{38}$$

$$(-in\Omega - \Omega_{kl})\langle a_k^\dagger a_l\rangle_n = -i\sum_{j\neq k;j\neq l}(g_{lj}\langle a_k^\dagger a_j\rangle_n - g_{jk}\langle a_j^\dagger a_l\rangle_n) - ig_{lk}(\langle a_k^\dagger a_k\rangle_n - \langle a_l^\dagger a_l\rangle_n) - \frac{i\beta\eta_{kl}}{2}\langle a_k^\dagger a_l\rangle_{n+1} - \frac{i\beta\eta_{kl}^*}{2}\langle a_k^\dagger a_l\rangle_{n-1}. \tag{39}$$

The set of equations for the Fourier components can again be written in matrix form

$$\underline{\mathbb{L}}\underline{\boldsymbol{\psi}} = \underline{\boldsymbol{\kappa}} \tag{40}$$

when introducing the block vector

$$\underline{\boldsymbol{\psi}} = (\dots, \boldsymbol{\psi}_1, \boldsymbol{\psi}_0, \boldsymbol{\psi}_{-1}, \dots)^\mathsf{T}, \tag{41}$$

with

$$\boldsymbol{\psi}_n = (\langle a_1^\dagger a_1\rangle_n, \dots, \langle a_N^\dagger a_N\rangle_n, \langle a_1^\dagger a_2\rangle_n, \langle a_2^\dagger a_1\rangle_n, \dots, \langle a_1^\dagger a_N\rangle_n, \langle a_N^\dagger a_1\rangle_n, \langle a_2^\dagger a_3\rangle_n, \langle a_3^\dagger a_2\rangle_n, \dots, \langle a_2^\dagger a_N\rangle_n, \langle a_N^\dagger a_2\rangle_n, \dots \langle a_{N-1}^\dagger a_N\rangle_n, \langle a_N^\dagger a_{N-1}\rangle)_n^\mathsf{T}, \tag{42}$$

as well as the block vector

$$\underline{\boldsymbol{\kappa}} = (\dots, 0, 0, +2\kappa_1 n_1, \dots, +2\kappa_N n_N, 0, 0, \dots)^\mathsf{T}. \tag{43}$$

The block matrix $\underline{\mathbb{L}}$ then takes the form of a tridiagonal block matrix

$$\underline{\mathbb{L}} = \begin{pmatrix} \cdots & \cdots & \cdots & \cdots & \cdots \\ \cdots & \mathbb{M}_1 & \mathbb{G}^- & \mathbb{O} & \cdots \\ \cdots & \mathbb{G}^+ & \mathbb{M}_0 & \mathbb{G}^- & \cdots \\ \cdots & \mathbb{O} & \mathbb{G}^+ & \mathbb{M}_{-1} & \cdots \\ \cdots & \cdots & \cdots & \cdots & \cdots \end{pmatrix}, \tag{44}$$

with

$$\mathbb{M}_n = \begin{pmatrix} -in\Omega + 2\kappa_1 & 0 & \cdots & 0 & +ig_{12} & -ig_{21} & \cdots & 0 & 0 \\ 0 & -in\Omega + 2\kappa_2 & \cdots & 0 & -ig_{12} & ig_{21} & \cdots & \cdots & \vdots \\ \vdots & \cdots & \cdots & \cdots & \cdots & \cdots & \cdots & \cdots & \vdots \\ 0 & 0 & \cdots & -in\Omega + 2\kappa_N & 0 & 0 & \cdots & -ig_{N-1,N} & ig_{N,N-1} \\ -ig_{21} & ig_{12} & \cdots & 0 & -in\Omega - \Omega_{12} & 0 & \cdots & 0 & 0 \\ ig_{21} & -ig_{12} & \cdots & 0 & 0 & -in\Omega - \Omega_{21} & \cdots & 0 & 0 \\ \vdots & \cdots & \cdots & \cdots & \cdots & \cdots & \cdots & \cdots & \vdots \\ 0 & 0 & -ig_{3N} & ig_{3N} & \cdots & \cdots & \cdots & 0 & -in\Omega - \Omega_{N,N-1} \end{pmatrix}, \tag{45}$$

$$\mathbb{G}^+ = \frac{i\beta}{2}\mathrm{diag}(0, \dots, 0, \eta_{12}, -\eta_{12}, \dots, \eta_{N-1,N}, -\eta_{N-1,N}), \tag{46}$$

and $\mathbb{G}^-$ defined as the matrix obtained from $\mathbb{G}$ when complex conjugating η_{kl}. The different perturbation orders n can be obtained by using $2n+1$ subblocks in the matrix $\underline{\mathbb{L}}$. Note that even though we use the same notation as in the QLE approach, the vectors and matrices used are different and also have a different dimension. Here the dimensions of the block vectors and matrices are $N^2(2n+1)$ and $N^4(2n+1)^2 2$.

The mean heat flux (transferred power over one oscillation period) from oscillator k at temperature T_k to an oscillator l at temperature $T_l = 0$ K is defined by [42]

$$P_{k\to l} = \hbar\omega_l 2\kappa_l\langle a_l^\dagger a_l\rangle_0, \tag{47}$$

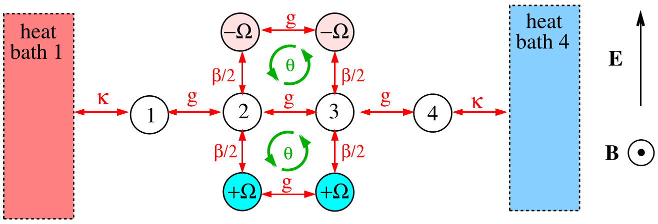

FIG. 2. Sketch of a chain of four resonators 1, 2, 3, and 4 with equal nearest-neighbor couplings g and resonance frequencies ω_0. The oscillators in the middle are modulated with a modulation strength β and a relative phase shift θ, resulting in synthetic electric and magnetic fields.

taking $n_i = 0$ for all other resonators. Again the total emitted mean power by oscillator k is given by

$$P_k^{\rm em} = \hbar\omega_k 2\kappa_k (n_k - \langle a_k^\dagger a_k\rangle_0) \tag{48}$$

and we have energy conservation, i.e., $P_k^{\rm em} = \sum_{l\neq k} P_{k\to l}$. The advantage of the QME approach is that, differently from the QLEs (30) and (31), a frequency integration is not necessary. On the other hand, the size of the matrices for a given perturbation order is much larger than for the QLE approach. Note also that the simplifying white-noise assumption in the QLE and QME approaches has the virtue that the cycle-averaged energy which is pumped into the system by the modulation is exactly zero. Hence any change in the power flowing between the oscillators or baths can be attributed to heat. (See Appendix C for a detailed discussion.)

V. FOUR RESONATORS CASE: NONRECIPROCAL HEAT FLUX WITH SYNTHETIC FIELDS

We consider here the heat flux in a chain of four resonators as depicted in Fig. 2. We assume that all resonators are identical and we further assume reciprocal nearest-neighbor coupling with identical coupling strength g so that the nonzero coupling constants are $g_{12} = g_{21} = g_{32} = g_{23} = g_{34} = g_{43} = g$. The resonance frequencies ω_1 and ω_4 of resonators 1 and 4 are fixed to ω_0, whereas the resonance frequencies of the resonators in the middle are modulated as

$$\omega_2 = \omega_0 + \beta\cos(\Omega t), \tag{49}$$

$$\omega_3 = \omega_0 + \beta\cos(\Omega t + \theta). \tag{50}$$

In this configuration, we first determine the power P_{14} transferred from resonator 1 to resonator 4 with $T_1 = 300$ K and $T_2 = T_3 = T_4 = 0$ K. Then we compare with the heat flow in the backward direction by calculating the power P_{41} transferred from resonator 4 to resonator 1 with $T_4 = 300$ K and $T_1 = T_2 = T_3 = 0$ K. Hence, only the first and the last resonator are in our configuration coupled to a heat bath. Therefore, here the modulation frequency Ω and the modulation strength β are in principle not limited by the constraint due to the white-noise assumption because the two resonators in the middle have zero temperature. Nonetheless, we will restrict ourselves to values which fulfill the above criteria for the white-noise approximation. For our numerical calculations we use $\omega_0 = 1.69\times10^{14}$ rad/s and $\kappa = 0.013\omega_0$, which are the values taken from those for a graphene flake

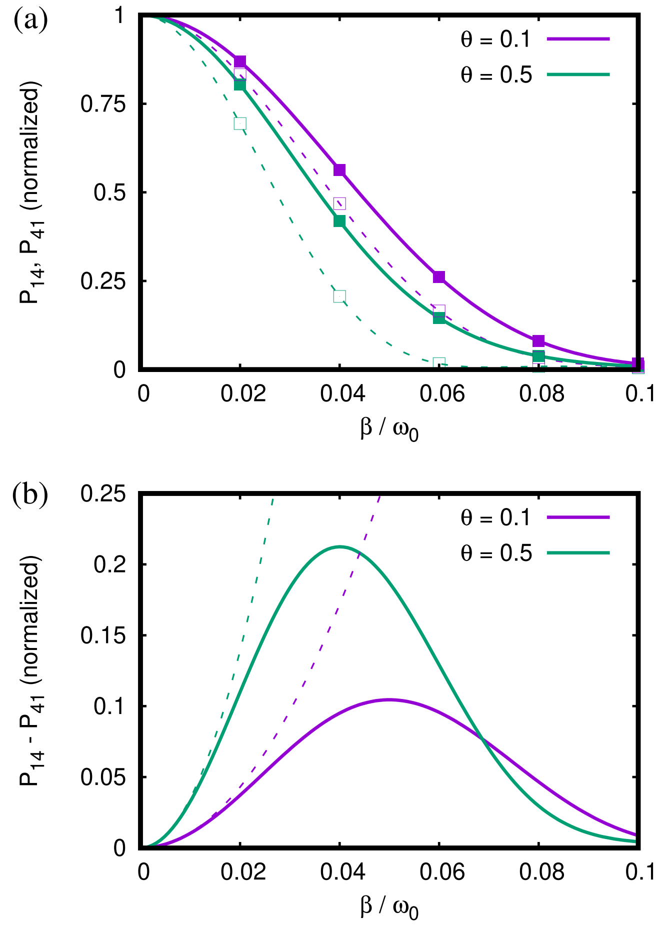

FIG. 3. Plot of (a) P_{14} (solid line) and P_{41} (dashed line) from the QME approach (47) at perturbation order $n = 15$ normalized to the value $P_{14}(\beta = 0) = P_{41}(\beta = 0) = 5.88\times10^{-22}$ W for $g = 0.011\kappa$ and $\Omega = 0.05\omega_0$ for $\theta = 0.1\pi$ and 0.5π. The closed and open symbols are the results for P_{14} and P_{41} from integration of spectra as in Fig. 5 from the QLE approach according to Eq. (31) at perturbation order $n = 10$. (b) Comparison of exact numerical results (solid lines) for the difference $P_{14} - P_{41}$ normalized to $P_{14}(\beta = 0) = P_{41}(\beta = 0) = 5.88\times10^{-22}$ W with the corresponding power difference from the approximate expression (dashed lines) from Eq. (52).

with $E_F = 0.4$ eV from Ref. [75]. The coupling constant g is determined by the near-field heat flux value, which depends on the relative distance between the graphene flakes. For a distance $d = 100$ nm between two graphene flakes, a fitting of the resonator model with the results from fluctuating electrodynamics [42] gives $g = 0.011\kappa$. Hence, we are in the weak-coupling regime.

In Fig. 3(a) we show the results for the transferred power as a function of the modulation strength β and for two different values of θ. We show the numerical results obtained with the QME method with Eq. (47) and the QLE approach with Eq. (31). First of all, we can see that both methods provide the same values for the exchanged power. Furthermore, it can be seen that the heat flux is clearly nonreciprocal, in contrast to the case of two resonators or two graphene flakes, where the heat flux is reciprocal despite the nonreciprocal spectra [42].

As detailed in Ref. [37], for instance, the nonreciprocity in transmission as sketched in Fig. 2 can be understood in second-order perturbation theory as an interference of different transmission paths. The energy at ω_0 provided by resonator 1 can go through the chain in second order via the upper and lower sidebands at $\omega_0 \pm \Omega$ by two scattering events $\omega_0 \to \omega_0 + \Omega$ and $\omega_0 + \Omega \to \omega_0$ or $\omega_0 \to \omega_0 - \Omega$ and $\omega_0 - \Omega \to \omega_0$, as sketched in Fig. 2. Due to the presence of the synthetic magnetic field, a phase is picked up in this process which is not the same in forward transmission from resonator 1 to resonator 4 and backward transmission from resonator 4 to resonator 1. This symmetry breaking of the synthetic magnetic field can be directly understood from Eq. (14), which shows that upward and downward transitions in the Floquet sidebands are connected to picking up a positive or negative phase. Hence the forward and backward transmission along the upper or lower sidebands results in different phase factors. We emphasize that when considering the heat flux between only two resonators, like our resonators 2 and 3 with modulation, there is no heat flux rectification due to the fact that because of the white-noise reservoirs the heat can enter via all the sidebands from resonator 2 to 3 or vice versa [42]. Here the rectification is achieved by adding two more resonators 1 and 4 which act as spectral filters for the energy entering resonator 2 from the left or 3 from the right so that the situation is very similar to the plane-wave transmission in Ref. [37]. For a plane wave with frequency ω being transmitted through the coupled resonators 2 and 3, the difference in the transmission is explicitly given by [37]

$$\tau_{23} - \tau_{32} = -2i\frac{\beta^2}{4}[\tau(\omega+\Omega) - \tau(\omega-\Omega)]\sin(\theta), \qquad (51)$$

where $\tau(\omega)$ is the transmission coefficient without modulation. This transmission coefficient shows that there is a nonreciprocal transmission for any phase difference $\theta \neq m\pi$ with integer m. From this expression it can be expected that at least in second-order perturbation theory, i.e., when β is sufficiently small, the largest difference can be expected for $\theta = \pi/2$. For the four-resonator configuration depicted in Fig. 2, a similar expression can be derived using a second-order perturbation theory for the QME approach as detailed in Appendix A. In the weak-coupling limit $g \ll \kappa$ we find for the difference of heat flux in the forward and backward directions

$$\frac{P_{14} - P_{41}}{\hbar\omega_0 n g} = \beta^2\frac{g^5}{\kappa^5}\left(\frac{7}{8}\frac{\mathrm{Im}(A^2)}{|A|^4} + \frac{\kappa\,\mathrm{Im}(A^3)}{|A|^6} - \frac{\kappa^3\mathrm{Im}(A^5)}{|A|^{10}}\right) \times \sin(\theta), \qquad (52)$$

where $A = 2\kappa - i\Omega$ and $n \equiv n_1 = n_4$ is the mean occupation number of the resonator 1 in the forward direction or resonator 4 in the backward direction. In Fig. 3(b) we compare its predictions with the exact numerical results from Fig. 3(a), clearly showing its validity in the small-β limit. This expression has a similar structure to Eq. (51), indicating the same dependence on θ in the limit of small driving amplitudes β. To see this effect, we show in Fig. 4 the relative power transmission

$$E \equiv \frac{P_{14} - P_{41}}{P_{14} + P_{41}}. \qquad (53)$$

It can be seen that indeed for $\beta < 0.05\omega_0$ the maximum difference in the forward and backward heat flow happens at $\theta = \pm\pi/2$. For larger modulation strengths higher-order

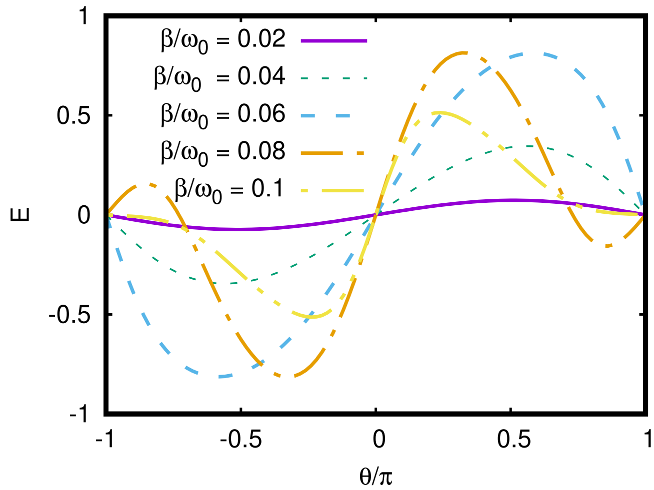

FIG. 4. Relative power transmission E defined in Eq. (53) as a function of the dephasing θ for $\Omega = 0.05\omega_0$ and different values of modulation strength β using the QME approach in order $n = 15$.

effects play a role, so this maximum shifts to slightly larger or smaller values of dephasing.

Finally, in Fig. 5 the spectra of power $P_{14,\omega}$ and power $P_{41,\omega}$ obtained with the QLE approach in the forward and backward directions are shown using $\Omega = 0.05\omega_0$, $\beta = 0.05\omega_0$, and $\theta = \pi/2$. It can be seen that the spectra for the heat flow in the forward and backward directions are not the same as also found for two graphene flakes only [42]. Furthermore, it can be seen that the sideband contribution is very small, so the main nonreciprocity stems from frequencies around the resonance ω_0. Integrating these spectra according to Eq. (31) gives the full transferred power for the forward and backward directions shown in Fig. 3(a).

Let us compare our results with the heat transport in other nonreciprocal systems, such as those in Refs. [31–33], where nonreciprocal heat flux between two nanoparticles is achieved

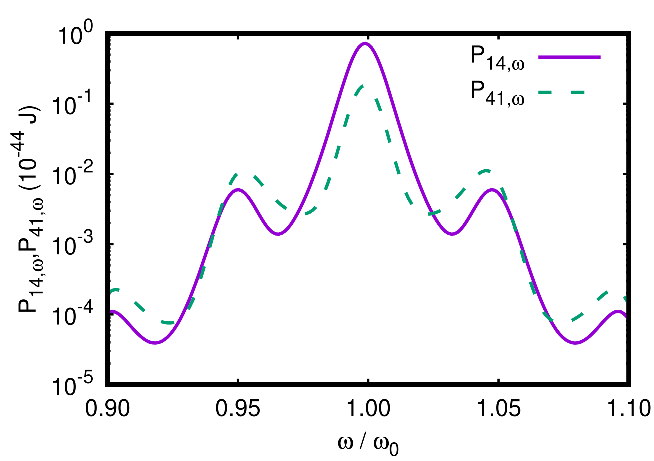

FIG. 5. Spectra for mean power $P_{14,\omega} = 2\kappa\hbar\omega_0\langle a_4^\dagger a_4\rangle_\omega$ for the forward heat flow and $P_{41,\omega} = 2\kappa\hbar\omega_0\langle a_1^\dagger a_1\rangle_\omega$ for the backward heat flow calculated from the spectra for the mean occupations numbers $\langle a_4^\dagger a_4\rangle_\omega$ and $\langle a_1^\dagger a_1\rangle_\omega$ in Eq. (29). The modulation parameters are $\Omega = 0.05\omega_0$, $\beta = 0.05\omega_0$, and $\theta = \pi/2$ and we use perturbation order $n = 10$.

by the heat transport via nonreciprocal surface waves of a nearby plasmonic substrate. In these systems the energy or heat flux rectification can be very efficient but at the cost of applying strong magnetic fields or using intrinsically nonreciprocal materials which do not allow for any active control of the rectification mechanism. In our system the rectification ratio expressed by the relative power transmission E can be close to one. We find for our choice of parameters at maximum a rectification ratio $R_1 = |P_{14} - P_{41}|/|P_{41}| = 8.6$ or $R_2 = |P_{14} - P_{41}|/\max|P_{41}|, |P_{12}| = 0.9$ in Fig. 4. The rectification ratio reported in Ref. [31] is $R_2 = 0.2$ for a magnetic field of 0.1 T and $R_2 \approx 0.9$ for a magnetic field of 1 T, whereas in Ref. [32] a rectification ratio $R_2 \approx 1$ or $R_1 \approx 249$ is achieved for a magnetic field of 2–3 T. By replacing the plasmonic substrate by a Weyl semimetal one can achieve even higher rectification ratios. Depending on the specific value of the momentum separation, parameter values of $R_1 = 2673$ or even larger were reported in Ref. [33]. However, Weyl semimetals do not allow for any active control of the nonreciprocal heat flux, whereas in our system the direction and the rectification strength can be controlled by the phase shift and modulation strength. Our rectification mechanism is also different from the modulation method in Ref. [56], where a nonreciprocal heat flux is observed for the heat flow through a specific triangular three-oscillator system by modulation of two of the three resonance frequencies with specific phase shifts and a modulation of the coupling strength between two of the three resonators. In that case, there are also significant pumped currents due to the modulation in the system, so a direct comparison is difficult. Depending on the choice of parameters, maximal relative power transmissions of $E \approx 0.5$ and even $E \approx 1$ are reported for cases without spectral filtering. This system is more complicated than ours in the sense that this system needs a dynamic modulation of the coupling strength and a frequency modulation including pump currents, whereas in our model only frequency modulations are needed.

Hence, in our four-resonator system we clearly find a nonreciprocal heat flow due to synthetic electric and magnetic fields. Even though our example might be difficult to realize in practice, it clearly shows that synthetic electric and magnetic fields can generate a nonreciprocal heat flux. We emphasize that this result is not limited to near-field heat transfer between graphene flakes but it is generally valid for any configuration and any heat transfer channel which can be described by four coupled resonators with synthetic fields.

VI. CONCLUSION

To summarize, based on the local QME, we have introduced a formalism for a QLE and a QME approach for N coupled resonators with synthetic electric and magnetic fields. Both approaches are equivalent and reproduce the same numerical results for the heat fluxes. However, the QLE approach is the natural choice when heat flux spectra are studied, whereas for the heat flow the QME approach is a better choice, because it is faster. As a very important example, we used both approaches to show, for a system of four linearly coupled resonators, that the heat flow is nonreciprocal when synthetic electric and magnetic fields are present. This is in contrast to the case of only two resonators where the heat flux is strictly reciprocal. We also verified numerically that both approaches give the same values for the heat flux. Even though for the numerical evaluation we considered the near-field heat transfer in a system of four coupled graphene flakes, our findings are very general and applicable to any system and any heat flux channel which can be described by coupled resonators. Hence, our formalism provides the fundament for further studies on heat flux and other physical effects in coupled many-resonator systems with synthetic fields.

ACKNOWLEDGMENTS

S.-A.B. acknowledges support from Heisenberg Programme of the Deutsche Forschungsgemeinschaft (DFG) under Project No. 461632548. S.-A.B. and P.R.-L. are grateful to the University of Montpellier and the group Theory of Light-Matter and Quantum Phenomena of the Laboratoire Charles Coulomb for hospitality in Montpellier where parts of this work were done. S.-A.B., P.R.-L., and M.A. acknowledge the QuantUM program of the University of Montpellier. G.S.A. is grateful for support from the Air Force Office of Scientific Research (Award No. FA9550-20-1-0366) and the Robert A. Welch Foundation (Grant No. A-1943). P.R.-L. acknowledges support from AYUDA PUENTE, URJC.

APPENDIX A: PERTURBATION THEORY FOR THE QME APPROACH

In this Appendix we derive the second-order expression in Eq. (52). To this end, we start with Fourier equations for the QME (40) taking terms with $n = 0, 1, -1$. Then we have

$$\mathbb{M}_0\boldsymbol{\psi}_0 = \boldsymbol{\kappa} - \mathbb{G}^+\boldsymbol{\psi}_{+1} - \mathbb{G}^-\boldsymbol{\psi}_{-1}, \tag{A1}$$

$$\mathbb{M}_{+1}\boldsymbol{\psi}_{+1} = -\mathbb{G}^+\boldsymbol{\psi}_2 - \mathbb{G}^-\boldsymbol{\psi}_0, \tag{A2}$$

$$\mathbb{M}_{-1}\boldsymbol{\psi}_{-1} = -\mathbb{G}^+\boldsymbol{\psi}_0 - \mathbb{G}^-\boldsymbol{\psi}_{-2}. \tag{A3}$$

By inserting the expressions for $\boldsymbol{\psi}_{+1/-1}$ into the equation for $\boldsymbol{\psi}_0$ and neglecting terms from $|n| \geqslant 2$ we arrive at

$$\mathbb{N}\boldsymbol{\psi}_0 = \boldsymbol{\kappa} \Rightarrow \boldsymbol{\psi}_0 = \mathbb{N}^{-1}\boldsymbol{\kappa}, \tag{A4}$$

with

$$\mathbb{N} = \left[\mathbb{M}_0 - \mathbb{G}^+\mathbb{M}_{+1}^{-1}\mathbb{G}^- - \mathbb{G}^-\mathbb{M}_{-1}^{-1}\mathbb{G}^+\right]. \tag{A5}$$

By defining

$$\mathbb{G}^+ = \frac{i\beta}{2}\tilde{\mathbb{G}}, \quad \mathbb{G}^- = \frac{i\beta}{2}\tilde{\mathbb{G}}^*, \tag{A6}$$

with $\tilde{G} = \mathrm{diag}(0, \dots, 0, \eta_{12}, -\eta_{21}, \dots, \eta_{N-1,N}, -\eta_{N-1,N})$, we have

$$\mathbb{N} = \left(\mathbb{M}_0 + \frac{\beta^2}{4}\left(\tilde{\mathbb{G}}\mathbb{M}_{+1}^{-1}\tilde{\mathbb{G}}^* + \tilde{\mathbb{G}}^*\mathbb{M}_{-1}^{-1}\tilde{\mathbb{G}}\right)\right). \tag{A7}$$

From this expressions it becomes more obvious that the first nonvanishing contributions to the zeroth order are stemming from the second-order terms, i.e., there is no contribution linear in β.

For the tight-binding model of the four identical resonators the involved vectors have 16 components and the matrices have a size of 16×16. By definition of $\boldsymbol{\psi}_0$ we are interested

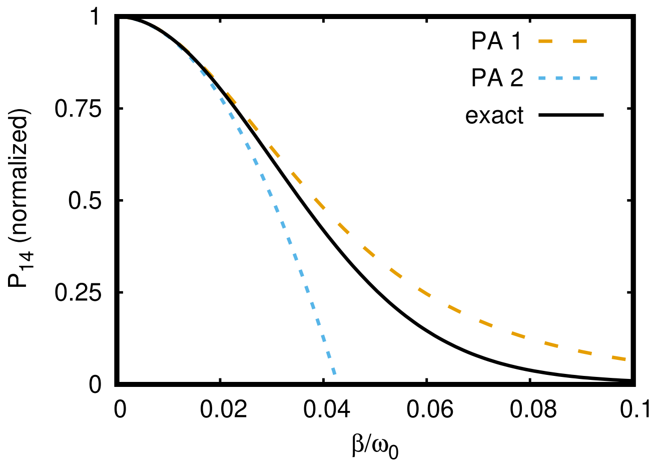

FIG. 6. Comparison of exact numerical results for P_{14} (black lines) with the second-order perturbation approach from Eq. (A7) (PA 1) and with those from Eq. (A8) (PA 2) using the same parameters as in Fig. 3(a) and $\theta = \pi/2$. The approximations for P_{41} are similar (not shown).

in the terms $\mathbb{N}^{-1}_{14}$ and $\mathbb{N}^{-1}_{41}$, which determine the transferred power $P_{4\to1}$ and $P_{1\to4}$. Obviously, there can only be nonreciprocity if $\mathbb{N}^{-1} \neq (\mathbb{N}^{-1})^T$. From the equation for $\mathbb{N}$ it can be seen that due to the phase terms $\tilde{\mathbb{G}}$ and $\tilde{\mathbb{G}}^*$ in the second-order contribution, in general, we have $\mathbb{N} \neq \mathbb{N}^T$, so also $P_{4\to1} \neq P_{1\to4}$ in general. Hence, the synthetic magnetic field results in an asymmetry for $\mathbb{N}$ and hence for $\mathbb{N}^{-1}$.

For small β we can further simplify the inverse of $\mathbb{N}$ as

$$\begin{aligned}\mathbb{N}^{-1} &= \left(\mathbb{M}_0 + \frac{\beta^2}{4}\left(\tilde{\mathbb{G}}\mathbb{M}_{+1}^{-1}\tilde{\mathbb{G}}^* + \tilde{\mathbb{G}}^*\mathbb{M}_{-1}^{-1}\tilde{\mathbb{G}}\right)\right)^{-1} \\ &= \left(\mathbb{1} + \frac{\beta^2}{4}\mathbb{M}_0^{-1}\left(\tilde{\mathbb{G}}\mathbb{M}_{+1}^{-1}\tilde{\mathbb{G}}^* + \tilde{\mathbb{G}}^*\mathbb{M}_{-1}^{-1}\tilde{\mathbb{G}}\right)\right)^{-1}\mathbb{M}_0^{-1} \\ &\approx \left(\mathbb{1} - \frac{\beta^2}{4}\mathbb{M}_0^{-1}\left(\tilde{\mathbb{G}}\mathbb{M}_{+1}^{-1}\tilde{\mathbb{G}}^* + \tilde{\mathbb{G}}^*\mathbb{M}_{-1}^{-1}\tilde{\mathbb{G}}\right)\right)\mathbb{M}_0^{-1}.\end{aligned} \tag{A8}$$

In Fig. 6 we show a comparison of the second-order results using Eqs. (A7) and (A8) with numerically exact results. As expected, the second-order expansion is only reliable for small enough values of β and the perturbation expression in Eq. (A7) is valid for a larger range than the perturbative expression in Eq. (A8).

Now we want to derive an analytical expression for the heat flux difference. Note that the heat flux difference for the forward and backward cases in our example is given by

$$P_{14} - P_{41} = 4\hbar\omega_0 n\kappa^2 \Delta N_{14}, \tag{A9}$$

where $\Delta N_{14} = \mathbb{N}^{-1}_{14} - \mathbb{N}^{-1}_{41}$ and $n \equiv n_1 = n_4$. That means we can focus on ΔN_{14} and add the prefactors later. Starting with the approximate expression in Eq. (A9) and making a Taylor expansion for $g \ll \kappa$, we obtain with *Mathematica* for ΔN_{14} the relatively long expression

$$\begin{aligned}\Delta N_{14} \approx \frac{\beta^2 g^2}{8|A_1|^6}\frac{g^4}{\kappa^4}\Bigg(&\frac{|A_1|^2\mathrm{Im}(A_1^2)}{A_0^3}\{4[\mathrm{Im}(\eta_{13}\eta_{12}^*) + \mathrm{Im}(\eta_{34}\eta_{24}^*)] + 3[\mathrm{Im}(\eta_{23}\eta_{13}^*) + \mathrm{Im}(\eta_{24}\eta_{23}^*)] + \mathrm{Im}(\eta_{14}\eta_{13}^*) + \mathrm{Im}(\eta_{24}\eta_{14}^*)\} \\ &+ \frac{\mathrm{Im}(A_1^3)}{A_0^2}[\mathrm{Im}(\eta_{14}\eta_{12}^*) + 2\,\mathrm{Im}(\eta_{24}\eta_{13}^*) + \mathrm{Im}(\eta_{34}\eta_{14}^*) - 3\,\mathrm{Im}(\eta_{12}\eta_{23}^*) - 3\,\mathrm{Im}(\eta_{23}\eta_{34}^*)] \\ &+ 2\frac{\mathrm{Im}(A_1^4)}{|A_1|^2 A_0}[\mathrm{Im}(\eta_{24}\eta_{12}^*) + \mathrm{Im}(\eta_{34}\eta_{13}^*)] - \frac{2\,\mathrm{Im}(A_1^5)}{|A_1|^4}\mathrm{Im}(\eta_{12}\eta_{34}^*)\Bigg),\end{aligned} \tag{A10}$$

where we have introduced $A_n = 2\kappa - in\Omega$. From this expression it can be seen that only for complex η_{ij} is there nonreciprocity. It can be further observed that there seem to be plenty of combinations which give a nonreciprocal heat flux. In our four-oscillator example resonator 3 is the only one with a nonzero phase $\theta \equiv \theta_3 \neq 0$ and resonators 1 and 4 are not modulated at all, so $\eta_{12} = -1$, $\eta_{14} = 0$, $\eta_{24} = 1$, $\eta_{34} = e^{i\theta} = -\eta_{13}$, and $\eta_{23} = 1 - e^{i\theta}$. With these specific values we get

$$\Delta N_{14} \approx \frac{\beta^2 g^6}{4\kappa^4}\sin(\theta)\left(\frac{7\,\mathrm{Im}(A_1^2)}{|A_1|^4 A_0^3} + \frac{4\,\mathrm{Im}(A_1^3)}{|A_1|^6 A_0^2} - \frac{\mathrm{Im}(A_1^5)}{|A_1|^{10}}\right). \tag{A11}$$

By adding the corresponding factors as defined in Eq. (A9) and realizing that $A_0 = 2\kappa$, we obtain the approximative analytical expression for the heat flux difference in Eq. (52).

APPENDIX B: DEFINITION OF HEAT FLUX

The heat flux between two oscillators k and l can be obtained by the rate of work done on oscillator k by l, which is classically defined by

$$P_{k\to l} = k_0(x_k - k_l)\dot{x}_k, \tag{B1}$$

where k_0 is the spring constant between the oscillators and x_k and x_l is their displacement. By taking the classical–quantum-mechanical correspondence and expressing the displacement and its temporal derivative by the quantum-mechanical creation and annihilation operators $a_k^\dagger$ and a_k, respectively, one can express the corresponding mean work rate by [38]

$$P_{k\to l} = -i\hbar\omega_k g_{lk}(\langle a_k a_l^\dagger\rangle - \langle a_l a_k^\dagger\rangle), \tag{B2}$$

where g_{kl} is the coupling constant between the oscillators. This expression can be generalized for the case where the coupling can be asymmetric to

$$P_{k\to l} = -i\hbar\omega_k(g_{lk}\langle a_k a_l^\dagger\rangle - g_{kl}\langle a_l a_k^\dagger\rangle). \quad \text{(B3)}$$

Now this work rate describes the heat flux when it is due to a temperature bias.

Instead of using the analogy with the work rate, the heat fluxes can also be directly determined from the QME. For instance, the power exchanged between all oscillators k with l can be defined as the mean change of the energy of oscillator l by [41]

$$\sum_{k\neq l} P_{k\to l} = -\frac{i}{\hbar}\langle[H_S, H_l]\rangle, \quad \text{(B4)}$$

with H_S defined in Eq. (2) and $H_k = \hbar\omega_k a_k^\dagger a_k$. This gives the expression (B3) for $P_{k\to l}$, validating the above reasoning. On the other hand, the power flowing between the reservoir k and the system is defined as [41,45]

$$P_k^{\rm em} = {\rm Tr}[D_k(\rho)H_k], \quad \text{(B5)}$$

where

$$D_k(\rho) = -\kappa_k(n_k+1)(a_k^\dagger a_k\rho_S - 2a_k\rho_S a_k^\dagger + \rho_S a_k^\dagger a_k) - \kappa_k n_k(a_k a_k^\dagger\rho_S - 2a_k^\dagger\rho_S a_k + \rho_S a_k a_k^\dagger) \quad \text{(B6)}$$

is the dissipator of the reservoir k and $H_k = \hbar\omega_k a_k^\dagger a_k$. Then we arrive at

$$P_k^{\rm em} = \hbar\omega_k 2\kappa_k(n_k - \langle a_k^\dagger a_k\rangle). \quad \text{(B7)}$$

Note that, due to Eq. (6), we have in steady state energy conservation in the form

$$\sum_{k\neq l} P_{k\to l} = P_k^{\rm em}. \quad \text{(B8)}$$

To determine the power flowing between two oscillators k and l we do not use the expression (B3), but we consider the heat flowing into the reservoir l due to a temperature bias in reservoir k, i.e., we assume that only reservoir k has nonzero temperature, which leads to the power transferred to reservoir l given by

$$P_{k\to l} = -P_l^{\rm em} = \hbar\omega_k 2\kappa_k\langle a_k^\dagger a_k\rangle. \quad \text{(B9)}$$

APPENDIX C: ENERGY PUMP DUE TO MODULATION

The power pumped into the system by the modulation can be quantified from Eq. (B7) using only the modulation terms from Eq. (13), so for each oscillator k we have

$$P_k^{\rm mod} = \hbar\beta m_k\cos(\Omega t+\theta_k)2\kappa_k(n_k - \langle a_k^\dagger a_k\rangle). \quad \text{(C1)}$$

We can compare this power input with that from the unmodulated part

$$P_k^{\rm unmod} = \hbar\omega_k 2\kappa_k(n_k - \langle a_k^\dagger a_k\rangle). \quad \text{(C2)}$$

Then it is obvious that

$$\frac{P_k^{\rm mod}}{P_k^{\rm unmod}} = \frac{\beta m_k}{\omega_k}\cos(\Omega t+\theta_k). \quad \text{(C3)}$$

Note that in the white-noise approximation the prefactor fulfills $\beta/\omega_k \ll 1$, so the power pumped into the system due to the modulation is negligibly small. In our model it can be shown that it is exactly zero.

To see that within the white-noise approximation the energy pumped into the system by the modulation is exactly zero, we first observe that by using the QLE (10) the change in the mean occupation number of each oscillator due to the modulation terms $m_k\beta\cos(\Omega t+\theta_k)$ from Eq. (13) is constant in time, i.e.,

$$\begin{aligned}\frac{d}{dt}\langle a_k^\dagger a_k\rangle_{\rm mod} &= \langle\dot a_k^\dagger a_k\rangle_{\rm mod} + \langle a_k^\dagger\dot a_k\rangle_{\rm mod}\\ &= im_k\beta\cos(\Omega t+\theta_k)\langle a_k^\dagger a_k\rangle\\ &\quad - im_k\beta\cos(\Omega t+\theta_k)\langle a_k^\dagger a_k\rangle\\ &= 0.\end{aligned} \quad \text{(C4)}$$

Similarly, we can use the definition of the system Hamiltonian $H_{\rm S}$ from Eq. (2) with the modulation in Eq. (13) to show that

$$\begin{aligned}\frac{d}{dt}\langle a_k^\dagger a_k\rangle_{\rm mod} &= -\frac{i}{\hbar}{\rm Tr}\big(\big[H_S^{\rm mod},\rho_S\big]a_k^\dagger a_k\big)\\ &= -\frac{i}{\hbar}\big\langle\big[a_k^\dagger a_k, H_S^{\rm mod}\big]\big\rangle\\ &= 0,\end{aligned} \quad \text{(C5)}$$

with

$$H_S^{\rm mod} = \sum_i \hbar\beta\cos(\Omega t+\theta_i)a_i^\dagger a_i. \quad \text{(C6)}$$

Hence, the energy of any oscillator, i.e., the energy of the full system of oscillators itself, is not changed by the modulation. This is in strong contrast to a modulation of the coupling strength as in Refs. [54–56], where the modulation introduces a strong pumping effect.

The full power emitted into the system by reservoir k with modulation per modulation cycle can also be expressed as

$$\begin{aligned}\overline{P}_k^{\rm em} &= \frac{2\pi}{\Omega}\int_{-\pi/\Omega}^{\pi/\Omega} dt\big(P_k^{\rm mod} + P_k^{\rm unmod}\big)\\ &= -\hbar\omega_k 2\kappa_k\langle a_k^\dagger a_k\rangle_0\\ &\quad - \hbar\beta m_k\kappa_k(\langle a_k^\dagger a_k\rangle_{-1}e^{i\theta_k} + \langle a_k^\dagger a_k\rangle_{+1}e^{-i\theta_k}),\end{aligned} \quad \text{(C7)}$$

using the Fourier series expansion from Eq. (35). The second line corresponds to the time-averaged contribution of the power input due to the modulation. This contribution is exactly zero due to the white-noise assumption, which results in $\langle a_k^\dagger a_k\rangle_{+1} = \langle a_k^\dagger a_k\rangle_{-1} = 0$, which can be inferred from Eq. (40). Hence, the energy pumped into the system is zero and using the expression

$$\overline{P}_k^{\rm em} = -\hbar\omega_k 2\kappa_k\langle a_k^\dagger a_k\rangle_0 \quad \text{(C8)}$$

quantifies the full power emitted into the system by reservoir k during one oscillation cycle.

[1] L. Hu, A. Narayanaswamy, X. Chen, and G. Chen, Appl. Phys. Lett. **92**, 133106 (2008).
[2] R. S. Ottens, V. Quetschke, S. Wise, A. A. Alemi, R. Lundock, G. Mueller, D. H. Reitze, D. B. Tanner, and B. F. Whiting, Phys. Rev. Lett. **107**, 014301 (2011).
[3] T. Kralik, P. Hanzelka, M. Zobac, V. Musilova, T. Fort, and M. Horak, Phys. Rev. Lett. **109**, 224302 (2012).
[4] M. Lim, S. S. Lee, and B. J. Lee, Phys. Rev. B **91**, 195136 (2015).
[5] J. I. Watjen, B. Zhao, and Z. M. Zhang, Appl. Phys. Lett. **109**, 203112 (2016).
[6] M. P. Bernardi, D. Milovich, and M. Francoeur, Nat. Commun. **7**, 12900 (2016).
[7] B. Song, D. Thompson, A. Fiorino, Y. Ganjeh, P. Reddy, and E. Meyhofer, Nat. Nanotechnol. **11**, 509 (2016).
[8] A. Fiorino, D. Thompson, L. Zhu, B. Song, P. Reddy, and E. Meyhofer, Nano Lett. **18**, 3711 (2018).
[9] R. Mittapally, J. W. Lim, L. Zhang, O. D. Miller, P. Reddy, and E. Meyhofer, Nano Lett. **23**, 2187 (2023).
[10] K. Ito, K. Nishikawa, A. Miura, H. Toshiyoshi, and H. Iizuka, Nano Lett. **17**, 4347 (2017).
[11] A. Fiorino, D. Thompson, L. Zhu, R. Mittapally, S.-A. Biehs, O. Bezencenet, N. El-Bondry, S. Bansropun, P. Ben-Abdallah, E. Meyhofer, and P. Reddy, ACS Nano **12**, 5774 (2018).
[12] K. Ito, K. Nishikawa, and H. Iizuka, Appl. Phys. Lett. **108**, 053507 (2016).
[13] J. Kou and A. J. Minnich, Opt. Express **26**, A729 (2018).
[14] N. H. Thomas, M. C. Sherrott, J. Broulliet, H. A. Atwater, and A. J. Minnich, Nano Lett. **19**, 3898 (2019).
[15] K. Shi, Z. Chen, Y. Xing, J. Yang, X. Xu, J. S. Evans, and S. He, Nano Lett. **22**, 7753 (2022).
[16] I. Latella and P. Ben-Abdallah, Phys. Rev. Lett. **118**, 173902 (2017).
[17] R. M. Abraham Ekeroth, P. Ben-Abdallah, J. C. Cuevas, and A. García-Martin, ACS Photon. **5**, 705 (2018).
[18] M.-J. He, H. Qi, Y.-X. Su, Y.-T. Ren, Y.-J. Zhao, and M. Antezza, Appl. Phys. Lett. **117**, 113104 (2020).
[19] A. Ott, R. Messina, P. Ben-Abdallah, and S.-A. Biehs, J. Photon. Energy **9**, 032711 (2019).
[20] E. Moncada-Villa and J. C. Cuevas, Phys. Rev. B **103**, 075432 (2021).
[21] E. Moncada-Villa and J. C. Cuevas, Phys. Rev. B **106**, 235430 (2022).
[22] L. Ge, K. Gong, Y. Cang, Y. Luo, X. Shi, and Y. Wu, Phys. Rev. B **100**, 035414 (2019).
[23] H. Wu, Y. Huang, L. Cui, and K. Zhu, Phys. Rev. Appl. **11**, 054020 (2019).
[24] L. Zhu and S. Fan, Phys. Rev. Lett. **117**, 134303 (2016).
[25] A. Ott, P. Ben-Abdallah, and S.-A. Biehs, Phys. Rev. B **97**, 205414 (2018).
[26] M. G. Silveirinha, Phys. Rev. B **95**, 115103 (2017).
[27] C. Khandekar and Z. Jacob, New J. Phys. **21**, 103030 (2019).
[28] P. Ben-Abdallah, Phys. Rev. Lett. **116**, 084301 (2016).
[29] A. Ott, S.-A. Biehs, and P. Ben-Abdallah, Phys. Rev. B **101**, 241411(R) (2020).
[30] P. Doyeux, S. A. H. Gangaraj, G. W. Hanson, and M. Antezza, Phys. Rev. Lett. **119**, 173901 (2017).
[31] A. Ott, R. Messina, P. Ben-Abdallah, and S.-A. Biehs, Appl. Phys. Lett. **114**, 163105 (2019).
[32] A. Ott and S.-A. Biehs, Phys. Rev. B **101**, 155428 (2020).
[33] Y. Hu, H. Liu, B. Yang, K. Shi, M. Antezza, X. Wu, and Y. Sun, Phys. Rev. Mater. **7**, 035201 (2023).
[34] L. Fan, Y. Guo, G. T. Papadakis, B. Zhao, Z. Zhao, S. Buddhiraju, M. Orenstein, and S. Fan, Phys. Rev. B **101**, 085407 (2020).
[35] J. Dong, W. Zhang, and L. Liu, Appl. Phys. Lett. **119**, 021104 (2021).
[36] E. Lustig and M. Segev, Adv. Opt. Photon. **13**, 426 (2021).
[37] C. W. Peterson, W. A. Benalcazar, M. Lin, T. L. Hughes, and G. Bahl, Phys. Rev. Lett. **123**, 063901 (2019).
[38] S.-A. Biehs and G. S. Agarwal, J. Opt. Soc. Am. B **30**, 700 (2013).
[39] G. Barton, J. Stat. Phys. **165**, 1153 (2016).
[40] K. Sasihithlu and G. S. Agarwal, Nanophotonics **7**, 1581 (2018).
[41] G. De Chiara, G. Landi, A. Hewgill, B. Reid, A. Ferraro, A. J. Roncaglia, and M. Antezza, New J. Phys. **20**, 113024 (2018).
[42] S.-A. Biehs and G. S. Agarwal, Phys. Rev. Lett. **130**, 110401 (2023).
[43] F. Herz and S.-A. Biehs, Europhys. Lett. **127**, 44001 (2019).
[44] S.-A. Biehs, R. Messina, P. S. Venkataram, A. W. Rodriguez, J. C. Cuevas, and P. Ben-Abdallah, Rev. Mod. Phys. **93**, 025009 (2021).
[45] G. T. Landi, D. Poletti, and G. Schaller, Rev. Mod. Phys. **94**, 045006 (2022).
[46] N. Kalantar, B. K. Agarwalla, and D. Segal, Phys. Rev. E **103**, 052130 (2021).
[47] A. Purkayastha, A. Dhar, and M. Kulkarni, Phys. Rev. A **94**, 052134 (2016).
[48] H. Lira, Z. Yu, S. Fan, and M. Lipson, Phys. Rev. Lett. **109**, 033901 (2012).
[49] N. Chamanara, S. Taravati, Z.-L. Deck-Léger, and C. Caloz, Phys. Rev. B **96**, 155409 (2017).
[50] N. A. Estep, D. L. Sounas, J. Soric, and A. Alu, Nat. Photon. **10**, 923 (2014).
[51] L. D. Tzuang, K. Fang, P. Nussenzveig, S. Fan, and M. Lipson, Nat. Photon. **8**, 701 (2014).
[52] K. Fang, Z. Yu, and S. Fan, Phys. Rev. Lett. **108**, 153901 (2012).
[53] A. Ghanekar, J. Wang, S. Fan, and M. L. Povinelli, ACS Photon. **9**, 1157 (2022).
[54] S. Buddhiraju, W. Li, and S. Fan, Phys. Rev. Lett. **124**, 077402 (2020).
[55] H. Li, L. J. Fernández-Alcázar, F. Ellis, B. Shapiro, and T. Kottos, Phys. Rev. Lett. **123**, 165901 (2019).
[56] L. J. Fernández-Alcázar, R. Kononchuk, H. Li, and T. Kottos, Phys. Rev. Lett. **126**, 204101 (2021).
[57] R. Messina and P. Ben-Abdallah, Phys. Rev. B **101**, 165435 (2020).
[58] N. Li, P. Hänggi, and B. Li, Europhys. Lett. **84**, 40009 (2008).
[59] N. Li, F. Zhan, P. Hänggi, and B. Li, Phys. Rev. E **80**, 011125 (2009).
[60] I. Latella, R. Messina, J. M. Rubi, and P. Ben-Abdallah, Phys. Rev. Lett. **121**, 023903 (2018).
[61] S.-A. Biehs and P. Ben-Abdallah, Phys. Rev. B **106**, 235412 (2022).
[62] R. Messina, A. Ott, C. Kathmann, S.-A. Biehs, and P. Ben-Abdallah, Phys. Rev. B **103**, 115440 (2021).

[63] A. Bermudez, M. Bruderer, and M. B. Plenio, Phys. Rev. Lett. **111**, 040601 (2013).
[64] P. Doyeux, R. Messina, B. Leggio, and M. Antezza, Phys. Rev. A **95**, 012138 (2017).
[65] B. Leggio, P. Doyeux, R. Messina, and M. Antezza, Europhys. Lett. **112**, 40004 (2015).
[66] B. Leggio, R. Messina, and M. Antezza, Europhys. Lett. **110**, 40002 (2015).
[67] A. Rivas and M. A. Martin-Delgado, Sci. Rep. **7**, 6350 (2017).
[68] G. De Chiara and A. Imparato, Phys. Rev. Res. **4**, 023230 (2022).
[69] A. Hewgill, G. De Chiara, and A. Imparato, Phys. Rev. Res. **3**, 013165 (2021).
[70] J. H. Shirley, Phys. Rev. **138**, B979 (1965).
[71] G. S. Agarwal, *Quantum Optics* (Cambridge University Press, Cambridge, 2012).
[72] A. Rivas, A. D. K. Plato, S. F. Huelga, and M. B. Plenio, New J. Phys. **12**, 113032 (2010).
[73] A. Levy and R. Kosloff, Europhys. Lett. **107**, 20004 (2014).
[74] I. R. Senitzky, Phys. Rev. **161**, 165 (1967).
[75] S. Thongrattanasiri, F. H. L. Koppens, and F. J. G. de Abajo, Phys. Rev. Lett. **108**, 047401 (2012).